THE JOURNAL OF BIOLOGICAL CHEMISTRY VOL. 285, NO. 24, pp. 18769–18780, June 11, 2010

Phospho-regulated ACAP4-Ezrin Interaction Is Essential for Histamine-stimulated Parietal Cell Secretion*

Received for publication, March 30, 2010 Published, JBC Papers in Press, April 1, 2010, DOI 10.1074/jbc.M110.129007

Xia Ding[‡§1], Hui Deng[‡¶1], Dongmei Wang[‡], Jiajia Zhou[‡], Yuejia Huang[‡¶], Xuannv Zhao[‡], Xue Yu[‡], Ming Wang[‡], Fengsong Wang[‡¶], Tarsha Ward[¶], Felix Aikhionbare[¶], and Xuebiao Yao[‡2]

From the [‡]Anhui Key Laboratory of Cellular Dynamics and Chemical Biology, University of Science and Technology of China, Hefei 230027, China, the [§]Department of Internal Medicine, Beijing University of Chinese Medicine, Beijing 100029, China, and the [¶]Department of Physiology and Medicine, Morehouse School of Medicine, Atlanta, Georgia 30310

The ezrin-radixin-moesin proteins provide a regulated linkage between membrane proteins and the cortical cytoskeleton and also participate in signal transduction pathways. Ezrin is localized to the apical membrane of parietal cells and couples the protein kinase A activation cascade to the regulated HCl secretion. Our recent proteomic study revealed a protein complex of ezrin-ACAP4-ARF6 essential for volatile membrane remodeling (Fang, Z., Miao, Y., Ding, X., Deng, H., Liu, S., Wang, F., Zhou, R., Watson, C., Fu, C., Hu, Q., Lillard, J. W., Jr., Powell, M., Chen, Y., Forte, J. G., and Yao, X. (2006) *Mol. Cell Proteomics* 5, 1437–1449). However, knowledge of whether ACAP4 physically interacts with ezrin and how their interaction is integrated into membrane-cytoskeletal remodeling has remained elusive. Here we provide the first evidence that ezrin interacts with ACAP4 in a protein kinase A-mediated phosphorylation-dependent manner through the N-terminal 400 amino acids of ACAP4. ACAP4 locates in the cytoplasmic membrane in resting parietal cells but translocates to the apical plasma membrane upon histamine stimulation. ACAP4 was precipitated with ezrin from secreting but not resting parietal cell lysates, suggesting a phospho-regulated interaction. Indeed, this interaction is abolished by phosphatase treatment and validated by an *in vitro* reconstitution assay using phospho-mimicking ezrin^{S66D}. Importantly, ezrin specifies the apical distribution of ACAP4 in secreting parietal cells because either suppression of ezrin or overexpression of non-phosphorylatable ezrin prevents the apical localization of ACAP4. In addition, overexpressing GTPase-activating protein-deficient ACAP4 results in an inhibition of apical membrane-cytoskeletal remodeling and gastric acid secretion. Taken together, these results define a novel molecular mechanism linking ACAP4-ezrin interaction to polarized epithelial secretion.

The functions of an epithelium depend on the polarized organization of its individual epithelial cells. The acquisition of a fully polarized phenotype involves a cascade of complex events, including cell-cell adhesion, assembly of a lateral cortical complex, reorganization of the cytoskeleton, and polarized targeting of transport vesicles to the apical and basolateral membranes (1).

Ezrin is an actin-binding protein of the ezrin/radixin/moesin family of cytoskeleton-membrane linker proteins (2). Within the gastric epithelium, ezrin has been localized exclusively to parietal cells and primarily to the apical canalicular membrane of these cells (*e.g.* see Refs. 3 and 4). Our previous studies showed that gastric ezrin is co-distributed with the β-actin isoform *in vivo* (5) and preferentially bound to the β-actin isoform *in vitro* (6). Because of its cytolocalization and observed stimulation-dependent phosphorylation, it was postulated that ezrin couples the activation of protein kinase A (PKA)[3] to the apical membrane remodeling associated with parietal cell secretion (*e.g.* see Ref. 4). Recently, we have mapped the PKA phosphorylation site on ezrin and demonstrated the importance of the phospho-regulation of ezrin in gastric acid secretion (7). Using mouse genetics, Tamura *et al.* (8) demonstrated that knockdown ezrin in stomachs to <5% of the wild-type levels results in severe achlorhydria. In these parietal cells, H,K-ATPase-containing tubulovesicles failed to fuse with the apical membrane, suggesting an essential role of ezrin in tubulovesicle docking. However, it is still not clear how ezrin links the apical targeting of H,K-ATPase-containing tubulovesicle to the remodeling of apical membrane and cytoskeleton during the parietal cell activation.

ARF6 GTPase is a conserved regulator of membrane trafficking and actin-based cytoskeleton dynamics at the leading edge of migrating cells. A key determinant of ARF6 function is the lifetime of the GTP-bound active state, which is orchestrated by GTPase-activating protein (GAP) and GTP-GDP exchanging

* This work was supported, in whole or in part, by National Institutes of Health (NIH) Grants DK-56292 and CA132389 and NIH, National Center for Research Resources (NCRR), Grant UL1 RR025008 from the Clinical and Translational Science Award program. This work was also supported by Chinese Natural Science Foundation Grants 30500183 and 30870990 (to X. D.), 30900497 (to F. W.), and 90508002 and 90913016 (to X. Y.); Chinese Academy of Science Grants KSCX1-YW-R-65, KSCX2-YW-H-10, KSCX2-YW-R-195; Chinese 973 Project Grants 2006CB943603, 2007CB914503, and 2010CB912103; International Collaboration Grant 2009DFA31010 (to X. D.); and Technology grant 2006BAI08B01-07 (to X. D.); China National Key Projects for Infectious Disease Grant 2008ZX10002-021; a Georgia Cancer Coalition breast cancer research grant; Atlanta Clinical and Translational Science Award Chemical Biology Grant P20RR011104; and Anhui Province Key Project Grant 08040102005. The facilities used were supported in part by NCRR, NIH, Grant G12RR03034.

[1] Both authors contributed equally to this work.

[2] To whom correspondence should be addressed. E-mail: yaoxb@ustc.edu.cn.

[3] The abbreviations used are: PKA, protein kinase A; GAP, GTPase-activating protein; GFP, green fluorescent protein; MEM, minimal essential medium; SLO, Streptolysin O; AP, aminopyrine; PIPES, piperazine-*N*,*N*′-bis(2-ethanesulfonic acid); PBS, phosphate-buffered saline; IBMX, 3-isobutyl-1-methylxanthine; siRNA, small interfering RNA; GST, glutathione *S*-transferase; MBP, maltose-binding protein.

factor. Recent studies show that ARF6 is mainly located in the parietal cell within the gastric glands, and it relocates from the cytoplasm to the apical membrane of parietal cells upon stimulation of acid secretion (*e.g.* see Ref. 9). Significantly, overexpression of $ARF6^{Q67L}$, a mutant lacking GTP hydrolysis activity, in cultured gastric glands inhibits acid secretion. These results suggest that ARF6 regulates gastric acid secretion in parietal cells and that the GTP hydrolysis cycle of ARF6 is essential for the activation pathway. However, very little is known about the molecular mechanisms underlying ARF6-mediated parietal cell secretion. Our recent proteomic study has identified a novel ARF6 GTPase-activating protein ACAP4 essential for volatile membrane remodeling during cell migration (10).

To delineate the molecular function of PKA-mediated phosphorylation of ezrin in parietal cell secretion, we took advantage of our recent development of Streptolysin O-permeabilized gastric glands and assessed the requirement of phosphorylation of ezrin in parietal cell activation by the addition of recombinant ezrin and its mutants. Our studies demonstrate that phosphorylation of ezrin at Ser^{66} is critical for parietal cell activation. To identify the downstream signal linking ezrin phosphorylation and tubulovesicle trafficking, we express phospho-mimicking ezrin and non-phosphorylatable ezrin in the cultured parietal cells and isolate a novel ezrin-binding protein, ACAP4. Our studies indicate that ezrin directly binds to ACAP4 in a Ser^{66} phosphorylation-dependent manner and specifies the apical localization of ACAP4 upon the parietal cell activation. Overexpression of non-phosphorylatable ezrin diminishes apical localization of ACAP4 and effects an inhibition in parietal cell activation. We propose that ACAP4-ezrin interaction provides a link between tubulovesicle trafficking and apical membrane reorganization in parietal cell activation.

MATERIALS AND METHODS

Reagents—[^{14}C]Aminopyrine was obtained from PerkinElmer Life Sciences. Monoclonal antibody (JL-18) against recombinant GFP was purchased from Clontech (Palo Alto, CA), whereas ezrin antibody 4A5 was produced and described by Hanzel *et al.* (11). Anti-ACAP4 antibody was generated as described by Fang *et al.* (10). FLAG monoclonal antibody M2 was purchased from Sigma. Rhodamine-coupled phalloidin and Alexa Fluor 350-conjugated goat anti-rabbit IgG were purchased from Molecular Probes, Inc. (Eugene, OR). LipofectAmine2000 was obtained from Invitrogen.

DNA Construction—The development of bacterial expression vectors containing human ezrin fused to histidine was described previously (12). GFP-ezrin was constructed by ligating an EcoRI-SalI PCR-amplified ezrin cDNA into pEGFP-N1 (Clontech) as described previously (7). The ezrin deletion mutants were constructed by a standard PCR method as described (7). All constructs were sequenced in full.

Recombinant adenoviruses expressing GFP-tagged ACAP4 (wild-type and R469G mutant) were generated using the AdMax system (Microbix Biosystems), as we described previously (10). Briefly, ACAP4 cDNA was inserted into pEGFP-N1 to fuse with the GFP sequence. ACAP4-GFP sequence was then amplified by PCR and inserted into an AdMax shuttle vector pDC311, resulting in pDC311/ACAP4-GFP. By co-transfection of human embryonic kidney HEK293 cells with pDC311/ACAP4-GFP and pBHGloxDE1,3Cre (Microbix Biosystems, containing modified adenovirus type-5 genome) using the CellPhect Transfection kit (Amersham Biosciences), recombination between these two plasmids led to infectious virus production. A single viral colony was isolated, amplified, and titrated. Aliquots of virus were stored at −80 °C.

Isolation of Gastric Glands and Aminopyrine Uptake Assay—Gastric glands were isolated from New Zealand White rabbits as modified by Yao *et al.* (13). Briefly, the rabbit stomach was perfused under high pressure with PBS (2.25 mM K_2HPO_4, 6 mM Na_2HPO_4, 1.75 mM NaH_2PO_4, and 136 mM NaCl) containing 1 mM $CaCl_2$ and 1 mM $MgSO_4$. The gastric mucosa was scraped from the smooth muscle layer, minced, and then washed twice with minimal essential medium (MEM) buffered with 20 mM HEPES, pH 7.4 (HEPES-MEM). The minced mucosa was then digested with 15 mg of collagenase (Sigma). Intact gastric glands were collected from the digestion mixture after 20–25 min and then washed three times in HEPES-MEM. In all subsequent gland experiments (aminopyrine uptake assay), glands were resuspended at 5% cytocrit (v/v) in the appropriate buffer for final assay.

Stimulation of intact and Streptolysin O (SLO)-permeabilized rabbit gastric glands was quantified using the aminopyrine (AP) uptake assay as described by Ammar *et al.* (14). Briefly, intact glands in HEPES-MEM were washed two times by settling at 4 °C in ice-cold K buffer (10 mM Tris base, 20 mM HEPES acid, 100 mM KCl, 20 mM NaCl, 1.2 mM $MgSO_4$, 1 mM NaH_2PO_4, and 40 mM mannitol, pH 7.4). SLO was added to a final concentration of 1 μg/ml, and the glands (at 5% cytocrit) were mixed by inversion and then incubated on ice for 10 min. The glands were then washed twice with ice-cold K buffer to remove unbound SLO while the permeabilization was initiated by incubating gland suspension at 37 °C in K buffer solution containing 1 mM pyruvate and 10 mM succinate. The incubation of SLO with gastric glands on ice is critical to allow sufficient SLO molecules to bind to the surface of parietal cells but prevents SLO entry into the intracellular compartment for a notable effect. The preincubation procedure also avoids variations among the batches of SLO.

To evaluate the function of ezrin in parietal cell activation, we generated recombinant ezrin and its phospho-mimicking and non-phosphorylatable mutants in bacteria. Briefly, histidine fusion ezrin and its mutants were expressed in BL21 (DE3) bacteria and purified using an Ni^{2+}-nitrilotriacetic acid column as described (7). The fusion proteins were then eluted in PBS containing 100 mM imidazole and then applied to a gel filtration column (Econ-Pac 10 DG, Bio-Rad) to remove imidazole and exchange PBS buffer for K buffer. The recombinant proteins were estimated to be 95% pure by SDS-PAGE; major contaminants were degraded fragments of ezrin. Protein concentrations were determined by a Bradford assay (15).

Affinity Precipitation of ACAP4 and Ezrin—To characterize the interaction between ACAP4 and ezrin, a GST-tagged ACAP4 deletion mutant was used as an affinity matrix to isolate recombinant His-tagged ezrin mutant proteins ($ezrin^{S66A}$ and

ezrin^{S66D}), using a protocol described by Cao *et al.* (16). The beads were then washed with PBS three times, followed by boiling in 1× sample buffer. The samples were resolved on 6–16% gradient SDS-polyacrylamide gel and analyzed by Western blotting.

Preparation of Gastric Subcellular Fractions—Gastric subcellular fractions were prepared according to Yao *et al.* (17). All fractionation procedures were performed under ice-cold conditions. Briefly, the treated glands were rinsed once in homogenizing buffer containing 125 mM mannitol, 40 mM sucrose, 1 mM EDTA, and 5 mM PIPES-Tris (pH 6.7) and homogenized with a very tightly fitting Teflon pestle. The homogenate was centrifuged to produce a series of pellets: PO, 40 × *g* for 5 min (whole cells and debris); P_1, 4,000 × *g* for 10 min (plasma membrane-rich fraction); P_2, 14,500 × *g* for 10 min; P_3, 100,000 × *g* for 60 min (microsomes); and S_3, supernatant (cytosol). The pellets were resuspended in medium containing 300 mM sucrose, 0.2 mM EDTA, and 5 mM Tris (pH 7.4). The protein concentration in each individual subcellular fraction was assayed using bovine serum albumin as a standard (18).

Equivalent aliquots of sample were analyzed by SDS-PAGE. Samples (35 μg of protein) were applied to 7.5–9% polyacrylamide gels and subjected to electrophoresis. All gels were run in duplicate, one for protein staining and one for transblotting. Proteins in the gel were stained with 0.125% Coomassie Brilliant Blue R-250 in methanol/acetic acid/water (5:1:4). For immunoblotting, the proteins were electrophoretically transferred to nitrocellulose. The α-subunit of H,K-ATPase was probed with a monoclonal antibody and visualized using an ECL system.

For further characterization of ACAP4 interaction with H,K-ATPase-rich tubulovesicles, microsomes from the P_3 fraction were resuspended in medium containing 300 mM sucrose, 0.2 mM EDTA, and 5 mM Tris (pH 7.4) and loaded on the top of a stepwise gradient containing 20, 27, and 33% sucrose in 5 mM Tris (pH 7.4) as described previously (18).

As previous studies (19), H,K-ATPase was enriched in 20 and 27% sucrose gradient fractions, whereas Rab11 was enriched in both 20 and 27% sucrose gradient fractions in addition to the 33% sucrose gradient (20). Aliquots of P3 along with 20, 27, and 33% sucrose gradient fractions were separated by SDS-PAGE, followed by transblotting onto nitrocellulose membranes that were probed for H,K-ATPase, Rab11, and ACAP4.

Cell Culture and Transfection—Primary cultures of gastric parietal cells from rabbit stomach were produced and maintained as described (7). Separate cultures of parietal cells were transfected with plasmids encoding GFP-tagged wild type ezrin and/or deletion mutants using Lipofectamine 2000 (Invitrogen) according to the manufacturer's instructions. Briefly, 1 μg of DNA was incubated in 600 μl of Opti-MEM (antibiotic-free), whereas 6 μl of Lipofectamine 2000 was added and left at room temperature for 25 min. The cultured parietal cells (~3% cytocrit; 6-well plates) were washed once with Opti-MEM. The DNA-lipid mix was added to the plates and incubated for 4 h, followed by replacement of 1.5 ml of medium B. The transfected cells were then maintained in culture at 37 °C until used for protein expression, partition, immunoprecipitation, or immunofluorescence.

For validating the interaction between ACAP4 and ezrin, GFP-ezrin and FLAG-ACAP4 co-transfected parietal cells were harvested and lysed in 1.5 ml of Tris-buffered saline (20 mM Tris-Cl, pH 7.4, 150 mM NaCl, 2 mM EGTA, 0.1% Triton X-100) containing a proteinase inhibitor mixture. The cell lysates were clarified by using an Eppendorf centrifuge at 13,000 rpm for 10 min. The resulting supernatants were then incubated with 15 μg of GFP monoclonal antibody (JL-18) at room temperature for 2 h, followed by the addition of 10 μl of Protein A/G beads for an additional 1 h (Pierce). The beads were collected and washed with Tris-buffered saline before boiling in SDS-PAGE sample buffer. Immunoprecipitates were then fractionated by SDS-PAGE, and proteins were transferred onto nitrocellulose membrane for Western blotting analyses. The blot was first labeled with ezrin antibody 4A5 to verify efficiency of GFP immunoprecipitation. The blot was then stripped with SDS-PAGE sample buffer at 55 °C for 20 min, followed by validation of ACAP4 protein precipitated by GFP-ezrin using a FLAG monoclonal antibody, M2 (Sigma).

siRNA Treatment and Assay for Knockdown Efficiency—Double-stranded 19-nucleotide RNA duplex targeted to ACAP4 (siRNA 1, 5′-TCTCACACAGCACGATAAA-3′; siRNA 2, 5′-CAACAAGACCTATGAGACT-3′) (10) was purchased from Dharmacon Research Inc. (Boulder, CO). SMARTpool siRNA oligonucleotide targeted to ezrin was also ordered from Dhamacon. As a control, either a duplex targeting cyclophilin or scrambled sequence was used (21). In the trial experiments, different concentrations of siRNA oligonucleotides were used for different time intervals of treatment as detailed previously, whereas transfection efficiency was judged based on the uptake of FITC-conjugated oligonucleotides (21). In brief, cultured parietal cells were transfected with siRNA oligonucleotides or control scrambled oligonucleotides, whereas efficiency of this siRNA-mediated protein suppression was judged by Western blotting analysis.

In one set of experiments, aliquots of ACAP4 siRNA-treated *versus* scrambled siRNA-treated gastric parietal cells were subjected to [^{14}C]aminopyrine uptake assay as described previously (18).

Immunofluorescence Microscopy—For cytolocalization of exogenously expressed ezrin, cultured parietal cells were transfected with wild type GFP-ezrin and GFP-ezrin phospho-mutants (S66A and S66D) and maintained in MEM for 30–36 h. Some cultures were treated with 100 μM cimetidine to maintain a resting state; others were treated with the secretory stimulants 100 μM histamine plus 50 μM IBMX in the presence of SCH28080, a proton pump inhibitor (7). Treated cells were then fixed with 2% formaldehyde for 10 min and washed three times with PBS, followed by permeabilization in 0.1% Triton X-100 for 5 min. Prior to application of primary antibody, the fixed and permeabilized cells were blocked with 0.5% bovine serum albumin in PBS, followed by incubation of primary antibodies against ezrin (4A5) or GFP. The endogenous and exogenous ezrin proteins were labeled by a fluorescein isothiocyanate-conjugated goat anti-mouse antibody and counterstained with rhodamine-coupled phalloidin to visualize filamentous actin. Coverslips were supported on slides by grease pencil markings and mounted in Vectashield (Vector). Images were

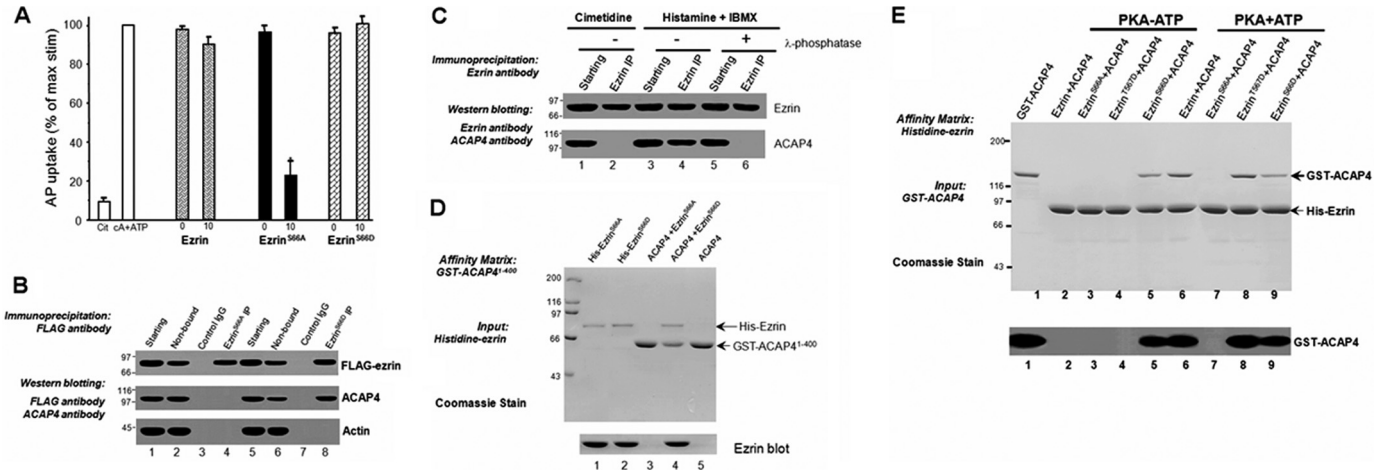

FIGURE 1. **Phosphorylation of Ser^{66} of ezrin specifies its association with ACAP4.** *A*, non-phosphorylatable ezrin^{S66A} inhibits acid secretion in SLO-permeabilized gastric glands. Glands were then stimulated with 100 μM cAMP plus 100 μM ATP, and the AP uptake was measured as described under "Materials and Methods." AP data are plotted as a percentage of the stimulated control for each experiment. *Error bars* represent S.E.; $n = 5$. *, significant difference from stimulated controls ($p < 0.05$). *B*, co-precipitation of FLAG-ezrin^{S66D}, but not FLAG-ezrin^{S66A}, with ACAP4 from transfected parietal cell cultures, as described under "Materials and Methods." Immunoprecipitates were fractionated by SDS-PAGE, followed by transferring onto nitrocellulose membrane for immunoblotting of FLAG-ezrin, ACAP, and actin. *C*, co-precipitation of endogenous ezrin-ACAP4 complex from stimulated, but not resting, gastric glands, as described under "Materials and Methods." Dephosphorylation of ezrin with λ-phosphatase treatment disrupts ezrin-ACAP4 complex isolated from stimulated glands. *D*, ACAP4 binds to Ser^{66}-phosphorylated ezrin via its N terminus. GST-ACAP4(1–400) was purified on glutathione-agarose beads and used as an affinity matrix for absorption of purified recombinant ezrin proteins (phospho-mimicking and non-phosphorylatable mutants). *Top*, SDS-polyacrylamide gel; *bottom*, Western blotting of ezrin. *E*, ACAP4-binding activity analysis of wild-type and mutant ezrin proteins in the presence of PKA alone (PKA-ATP; no phosphorylation) or PKA plus ATP (*PKA + ATP*; phosphorylation). *Top*, Coomassie Blue-stained SDS-polyacrylamide gel. ACAP4 binding was observed after incubation of ezrin with both PKA and ATP (*lane 6*) but not with PKA in the absence of ATP (*lane 2*). The addition of PKA on its own, without ATP, had no effect (not shown). In addition, the ACAP4 binding activity of ezrin^{S66A} and ezrin^{S66D} was unaffected by treatment of PKA and ATP (*lanes 7* and *9*). *Bottom*, Western blotting of ezrin.

taken on a Zeiss Axiovert-200 fluorescence microscope using a ×63, 1.3 numerical aperture PlanApo objective. Figures were constructed using Adobe Photoshop.

Confocal Microscopy—Immunostained parietal cells were examined under a laser-scanning confocal microscope LSM510 NLO (Carl Zeiss, Germany) scan head mounted transversely to an inverted microscope (Axiovert 200; Carl Zeiss) with a ×40, 1.0 numerical aperture PlanApo objective. Single images were collected by an average of 10 scans at a scan rate of 1 s/scan. Optical section series were collected with a spacing of 0.4 μm in the *z* axis through the ~12-μm thickness of the cultured parietal cells. The images from double labeling were simultaneously collected using a dichroic filter set with Zeiss image processing software (LSM 5, Carl Zeiss, Germany). Digital data were exported into Adobe Photoshop for presentation.

Western Blot—Samples were subjected to SDS-PAGE on 6–16% gradient gel and transferred onto nitrocellulose membrane. Proteins were probed by appropriate primary antibodies and detected using ECL (Pierce). The band intensity was then quantified using a PhosphorImager (Amersham Biosciences).

RESULTS

Phosphorylation of Ezrin at Ser66 Is Required for Parietal Cell Activation—The gastric parietal cell provides an excellent system to study ezrin function, where other ERM proteins are absent (see Refs. 22 and 23). We have recently established a permeable gland model that permits entry of relatively large molecular components (*e.g.* recombinant syntaxin proteins; see Refs. 14, 24, and 25). Our previous studies revealed that expression of S66A mutant ezrin in cultured parietal cells attenuates the dilation of apical vacuolar membrane associated with stimulation by histamine. To directly assess the role of ezrin in parietal cell acid secretion, we introduced recombinant full-length, phospho-mimicking, and non-phosphorylatable mutants into the SLO-permeabilized glands. Recombinant proteins, expressed in bacteria were purified to homogeneity using a Ni^{2+}-nitrilotriacetic acid column. Recombinant proteins were added to SLO-permeabilized glands in the presence and absence of cAMP/ATP as previously described (*e.g.* see Refs. 14 and 24). The addition of full-length ezrin caused relatively small changes in AP uptake (at most ~7% decrease), and there was no dose-dependent inhibitory effect. In contrast, non-phosphorylatable ezrin mutant caused a dose-dependent inhibition of acid secretion in SLO-permeabilized glands, as measured by AP uptake. No significant inhibition was noted at 2.5 μg of protein/ml (data not shown), but 5 μg of protein/ml caused a 23.9% reduction in acid secretion, and maximal inhibition (68–77%) occurred at 10 μg/ml (Fig. 1*A*). Interestingly, the addition of phospho-mimicking ezrin mutant caused relatively small changes in AP uptake (at most ~9.3% increase). These experiments support the notion that the phosphorylation of ezrin at Ser^{66} is required for parietal cell activation.

Phosphorylation of Ezrin at Ser^{66} Induces an Ezrin-ACAP4 Interaction—We reasoned that the inhibition seen in the SLO-permeabilized glands is due to a dominant effect exerted by the addition of a non-phosphorylatable ezrin mutant. Our previous studies show that exogenously expressed ezrin bears the same biochemical characteristics as those of endogenous protein (7). Because ezrin is localized to the apical membrane regardless of ezrin phosphorylation, we reasoned that phosphorylation of ezrin at Ser^{66} may be critical for associating proteins essential for acid secretion. To this end, cultured parietal cells were transiently transfected to express FLAG-tagged ezrin proteins

(non-phosphorylatable and phospho-mimicking), followed by immunoprecipitation using anti-FLAG affinity beads. The immunoprecipitated proteins were fractionated by SDS-PAGE, followed by transferring onto nitrocellulose membrane. As shown in Fig. 1*B*, Western blotting with an anti-FLAG antibody confirmed a successful isolation of FLAG-tagged ezrin from cultured parietal cells. Our recent study has identified a novel signaling complex containing ezrin, ARF6, and ACAP4 (10), so we first examined the presence of ACAP4 in the ezrin immunoprecipitates. To our surprise, ACAP4 is only present in the FLAG-ezrin^{S66D} immunoprecipitates (Fig. 1*B*, *lane 8*) and not ezrin^{S66A} immunoprecipitates, suggesting that ACAP4 may interact with ezrin in a Ser^{66} phosphorylation-dependent manner.

If ezrin interaction with ACAP4 depends on phosphorylation of Ser^{66}, histamine stimulation should promote ACAP4-ezrin interaction in gastric parietal cells, and phosphatase treatment should disrupt this interaction. Indeed, immunoprecipitation of ezrin brought down ACAP4 from histamine-stimulated parietal cells (Fig. 1*C*, *lane 4*) but not cimetidine-treated parietal cells (*lane 2*). Treatment of parietal cell lysates from histamine-stimulated preparation with λ-phosphatase prevented the co-precipitation of ACAP4 with ezrin. Thus, we conclude that phosphorylation of ezrin at Ser^{66} orchestrates ezrin-ACAP4 interaction.

To ascertain if ezrin physically interacts with ACAP4, we sought to carry out a pull-down assay using bacterially recombinant proteins. To this end, we attempted to generate a GST fusion protein containing full-length ACAP4 and its deletion mutants (ACAP4(1–400) and ACAP4(401–903)) and immobilized these fusion proteins on agarose beads, mixed with bacterially recombinant ezrin proteins (His-ezrin^{S66A} and His-ezrin^{S66D}). After extensive washing, proteins bound to the beads were eluted and fractionated by SDS-PAGE. As shown in Fig. 1*D*, Coomassie Blue staining shows that ezrin binds to the first 400 amino acids of ACAP4. The affinity matrix, which had immobilized the C-terminal ACAP4 did not retain any ezrin (data not shown), indicating that the N-terminal 400 amino acids mediate the interaction of ACAP4 with phospho-mimicking ezrin. Thus, we concluded that the first 400 amino acids of ACAP mediate the physical contact between ACAP4 and ezrin^{S66D}.

To eliminate a potential artifact of using mutant proteins, we assessed ACAP4 binding after *in vitro* phosphorylation of wild-type ezrin by PKA. In addition, we also included the non-phosphorylatable ezrin^{S66A} mutant to probe if other PKA-phosphorylation sites may also be involved in ACAP4-ezrin interaction. As shown in Fig. 1*E*, a dramatic increase in ACAP4 binding was observed after incubation of ezrin with both PKA and ATP (*lane 6*) but not with PKA in the absence of ATP (*lane 2*). The addition of ATP on its own, without PKA, had no effect (not shown). In addition, the ACAP4-binding activity of ezrin^{S66A} and ezrin^{S66D} was unaffected by treatment with PKA and ATP (*lanes 7* and *9*). On the other hand, the phospho-mimicking mutant of ezrin^{T567D} did not exhibit any ACAP4-binding activity with PKA in the absence of ATP (*lane 4*). However, a dramatic increase in ACAP4 binding was observed after incubation of ezrin^{T567D} with both PKA and ATP (*lane 8*). Western blotting analyses of ezrin validated the Ser^{66} phosphorylation-mediated ACAP4-ezrin interaction (*bottom*). Thus, phosphorylation of ezrin by PKA directly modulates the ACAP4 binding activity of ezrin. These results suggest that promotion in ACAP4 binding affinity of ezrin after phosphorylation of Ser^{66} may contribute to the physiological regulation of ezrin function *in vivo*.

Histamine Stimulation of Acid Secretion Induces Translocation of ACAP4—During the active secretory processes, the apical and canalicular plasma membranes of parietal cells undergo a major membrane-cytoskeleton remodeling due to the fusion of tubulovesicles. Therefore a shift in the distribution of the H,K-ATPase activity by histaminergic stimuli has proved to be a valid index to judge the membrane transformation during acid secretion in isolated gastric glands (21, 24) (schematic drawing shown in Fig. 2*A*). To test whether histamine stimulation induces relocation of ACAP4 in gastric glands, we carried out membrane fractionation experiments on glands maintained in the resting state (100 μM cimetidine) and glands that were maximally stimulated (100 μM histamine plus 50 μM IBMX). Homogenates of the variously treated gland preparations were separated by differential centrifugation, and cell fractions were assayed for H,K-ATPase content for validating the stimulation of acid secretion. The stimulation-associated redistribution of H,K-ATPase protein was assessed using SDS-PAGE and Western blotting. Coomassie Blue-stained SDS gels are shown in Fig. 2*B*. Except for the region of ~95 kDa (region of the α-subunit of H,K-ATPase), there was very little difference between the resting and stimulated preparations for the pattern of protein distribution within a given cellular fraction, consistent with our earlier observation (17).

To verify that the 95-kDa polypeptide was the α-subunit of H,K-ATPase, proteins were transferred onto nitrocellulose and probed with an antibody against the α-subunit of H,K-ATPase. It is clear from the blot shown in Fig. 2*C* (*top*) that H,K-ATPase protein content in the P_1 of histamine-stimulated glands is higher than that of cimetidine-treated glands. Although the ezrin levels were not changed in any given fractions between resting and stimulated preparations (*bottom*), it is clear from the blot shown in the *middle* that ACAP4 content in the P_1 of histamine-stimulated glands is higher than that of cimetidine-treated glands (*middle*), similar to what was observed for the H,K-ATPase distribution pattern. These data clearly support the conclusion that ACAP4 content is redistributed from the microsomal fraction to the apical membrane-rich fraction in response to histamine stimulation of parietal cell secretion. Additional sucrose gradient sedimentation assay demonstrated that ACAP4 is tightly associated with H,K-ATPase-rich vesicles.

Because ezrin is a part of the apical polarity determinant protein complex, biochemical interaction between ezrin and ACAP4 and the histamine-induced translocation profile led us to test whether ACAP4 is an apically distributed protein in secreting parietal cells. Fig. 2*D* (*a–c*) shows optical sections from non-secreting (cimetidine) parietal cells. Similar to what has been noted in earlier studies, ezrin is localized to the plasma membranes, most prominently to the apical membrane vacuoles that have been sequestered into the cell interior as rings

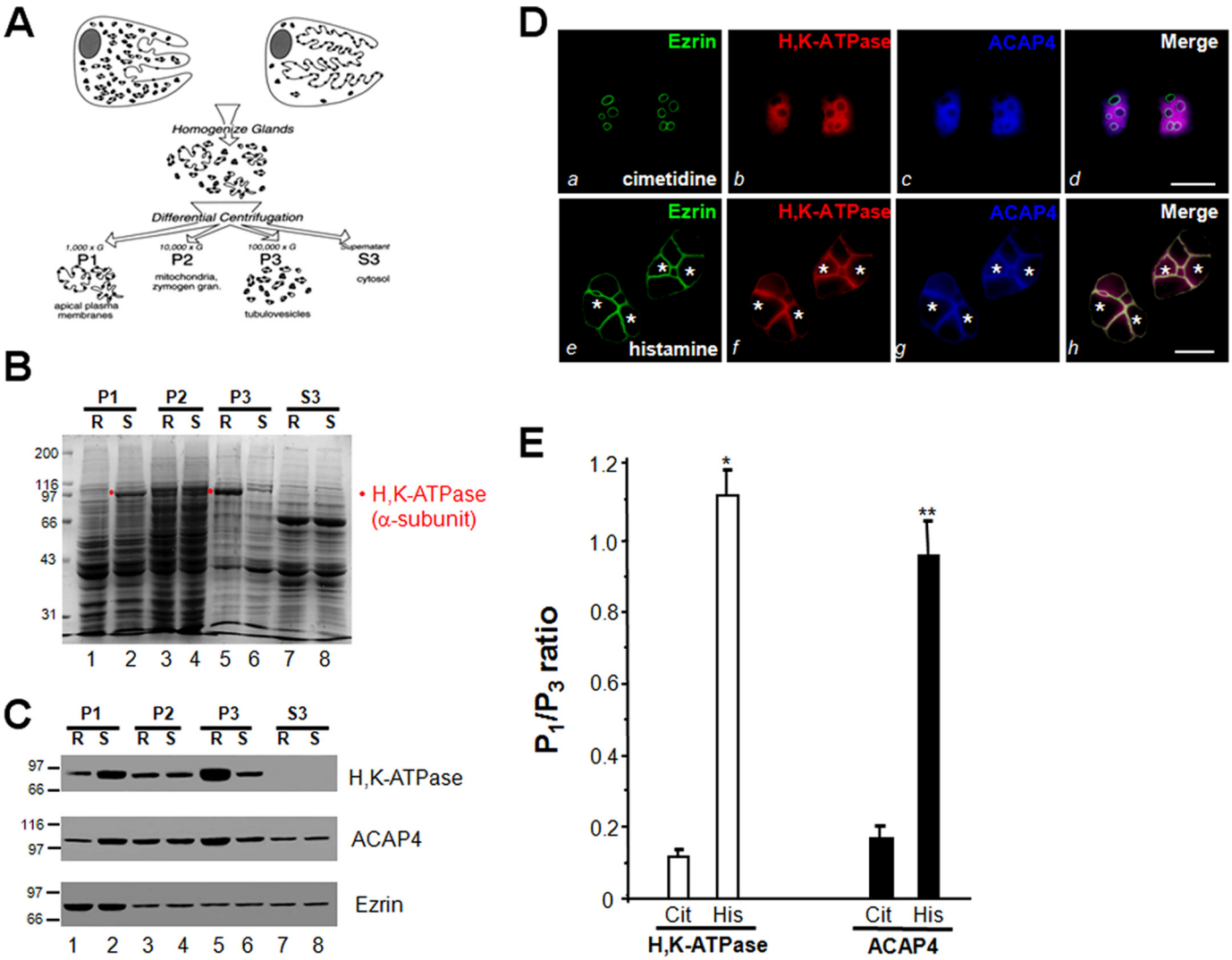

FIGURE 2. **Histamine stimulation triggers the redistribution of ACAP4 to the apical membrane of parietal cells.** *A*, schematic diagram of subcellular fractionation of resting and stimulated gastric glands. *B*, SDS-PAGE of subcellular fractions from resting (*R*) and stimulated (*S*) gastric gland preparations. Equal total proteins (35 μg/lane) were used. *C*, Western blotting analyses of ezrin, ACAP4, and H,K-ATPase (α-subunit) of subcellular fractions derived from resting and stimulated gastric glands. Note that stimulation enriches the protein levels of H,K-ATPase and ACAP4 in P_1 fraction. *D*, this montage represents confocal images collected from resting and secreting gastric parietal cells triply stained for ezrin (*green*), H,K-ATPase (*red*), ACAP4 (*blue*), and their *merged images*. Ezrin is mainly located in the apical plasma membrane of parietal cells (seen as *rings*) in a pattern suggestive of the apical plasma membrane invaginations that form the intracellular canaliculi (*a*). Labeling of ACAP4 is mainly located in the cytoplasm of parietal cells (*c*), which is mainly co-localized to that of H,K-ATPase distribution (*b*; *red*), whereas a lesser degree of co-localization is seen in apical membrane. Their apical localization becomes readily evident when the three images are merged (*d*; *white*). *Bar*, 15 μm. Stimulation induces remodeling of the apical membrane, seen as a dilation of apical vacuoles in the parietal cells (*e–g*). Labeling of ACAP4 is mainly located in the dilated apical vacuole membrane (*g*, *asterisk*), which is superimposed onto that of ezrin distribution in the *merge* (*h*). *Bar*, 15 μm. *E*, densitometric quantitation of the α-subunit of H,K-ATPase and ACAP4 proteins from P_1 (plasma membrane-enriched) and P_3 (tubulovesicle-enriched) fractions. The measurements were expressed as P_1/P_3 ratio. All data are given as means ± S.E. (*error bars*) of four preparations. *Cit*, cimetidine; *His*, histamine.

(*a*; *green*). ACAP4 staining appears as cytoplasmic but concentrated near the apical membrane vacuoles (*c*; *blue*), which is similar to the distribution profile of H,K-ATPase (*b*; *red*). However, there is very little co-localization of ACAP4, H,K-ATPase, and ezrin to the apical membrane, as can be seen in the merged image from three channels (*d*, *white*).

The stimulation of parietal cell acid secretion involves insertion of H,K-ATPase-containing tubulovesicle membrane into apical canalicular membrane, resulting in dilation of apical membrane vacuoles as active HCl and water transport occurs (*e.g.* 7). Because of this swelling, stimulated parietal cells are considerably larger in diameter than their resting counterparts (*e.g.* see Ref. 7). Because a portion of ACAP4 is co-distributed with ezrin to the apical membrane of resting cells, we tested if ACAP4 and ezrin remain co-localized as the apical cytoskeletal remodeling occurs. Fig. 2*D* (*a′–d′*) shows optical sections taken from parietal cells treated with the secretagogues histamine plus IBMX and probed for ACAP4, H,K-ATPase, and ezrin, respectively. In secreting cells, the dilated apical canalicular vacuoles occupy most of the cytoplasmic space, due to the recruitment of H,K-ATPase, as noted in our earlier studies (*e.g.* see Ref. 7). Compared with what was seen in resting parietal cells (*a–c*), the majority of ACAP4 is concentrated and co-localized with ezrin at the apical membrane of secreting cells (Fig. 2*D*, *g*), consistent with the fact that PKA-mediated phosphorylation promotes the ezrin-ACAP4 interaction (*e.g.* see Ref. 7).

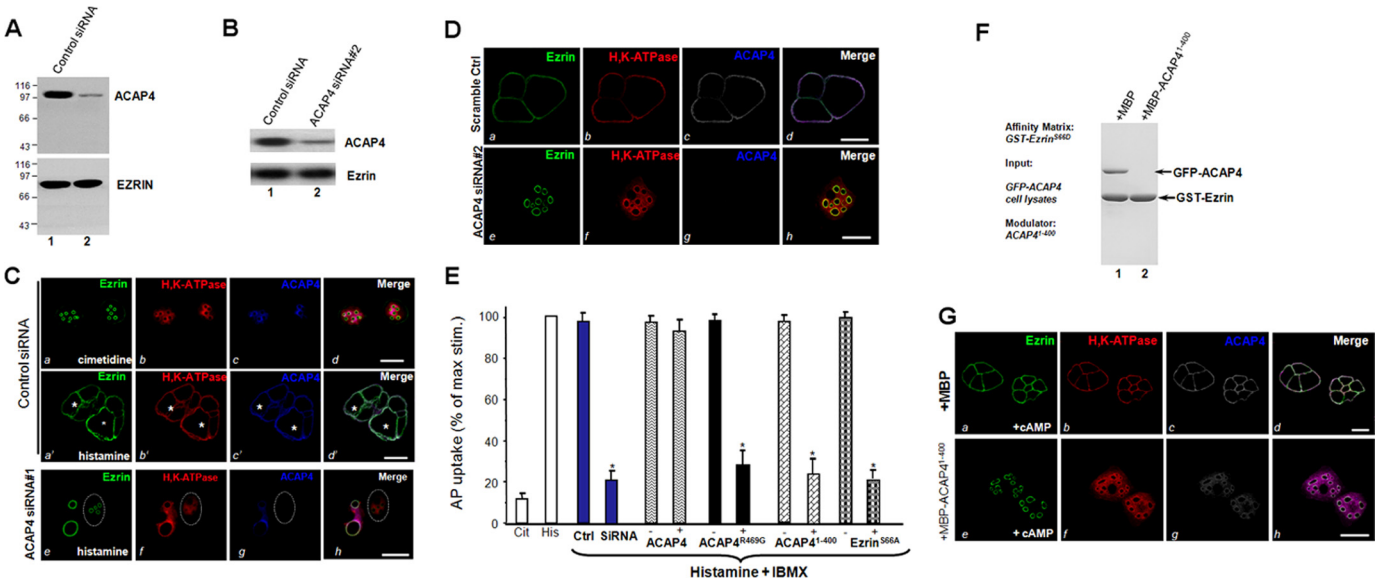

FIGURE 3. **ACAP4 is essential for parietal cell acid secretion.** *A* and *B*, parietal cells were transfected with the ACAP4 siRNA oligonucleotides for 48 h and subjected to SDS-PAGE and immunoblotting. *Left*, immunoblot for ACAP4; *right*, immunoblot for ezrin. Scrambled oligonucleotides were used as controls. *C* and *D*, these two sets of confocal images were collected from resting and secreting gastric parietal cells triply stained for ezrin (*green*), H,K-ATPase (*red*), and ACAP4 (*blue*). Ezrin is mainly located in the apical vacuole membrane of parietal cells, which was seen as *rings* in control siRNA-treated cells (*a*). Stimulation of control siRNA-treated parietal induces a dilation of apical vacuole membrane (*a′*). However, suppression of ACAP4 (siRNA 1 and siRNA 2) by siRNA abolishes the apical concentration of H,K-ATPase (*f*) but not ezrin (*e*). In addition, knockdown of ACAP4 attenuates the dilation of apical vacuoles (*c′ versus g*; *circled*). *Bar*, 15 μm. *E*, inhibition of parietal cell secretion by GAP-deficient ACAP4. Cultured parietal cells were infected by adenovirus-containing wild type and mutant ACAP4 for 2 h before stimulation with histamine and IBMX, and AP uptakes were measured. AP uptakes are shown for resting and stimulated controls and for stimulated glands treated with either full-length ACAP or ACAP4 mutants or ezrin^{S66D} mutant. AP data are plotted as a percentage of the stimulated control for each experiment. *Error bars*, S.E. ($n = 4$ for all experiments). In a separate preparation, aliquots of cultured parietal cells were transfected with ACAP4 siRNA and scrambled oligonucleotides followed by a standardized AP uptake assay. *, $p < 0.01$ compared with stimulated controls. *max stim*, maximal stimulation. *F*, addition of ACAP4(1–400) recombinant protein disrupts ezrin-ACAP4 association. Purified GST-ezrin^{S66D} protein on glutathione-Sepharose beads were used as an affinity matrix for absorbing GFP-ACAP4. After extensive washes, aliquots of ACAP4-bound GST-ezrin^{S66D}-Sepharose beads were incubated with 5 μM purified ACAP4(1–400) protein on a rotator for 30 min at room temperature. After extensive washes, the Sepharose beads were boiled in SDS-PAGE sample buffer, and bound proteins were fractionated by SDS-PAGE, followed by visualization in Coomassie Blue stain. Note that incubation of ACAP4(1–400) peptide with ACAP4-bound GST-ezrin^{S66D}-Sepharose beads disrupts ezrin-ACAP4 interaction. *G*, ezrin-ACAP4 is essential for apical translocation of ACAP4 and H,K-ATPase. To directly assess the role of ACAP4-ezrin interaction in parietal cell activation, recombinant ACAP4(1–400) protein was introduced into SLO-permeabilized cells, followed by the addition of cAMP/ATP. Twenty minutes after the treatment, cultured parietal cells were then fixed for immunocytochemistry. Stimulation of SLO-permeabilized cells with cAMP plus ATP induced a dilation of apical vacuole membrane in the presence of MBP protein (*a–d*). However, the addition of ACAP4(1–400) peptide abolishes the apical concentration of H,K-ATPase (*f*) and ACAP4 (*g*) but not ezrin (*e*). *Bar*, 15 μm.

To quantify the translocation of ACAP4 and α-subunit of H,K-ATPase and ACAP4 in response to histamine stimulation, we carried out densitometric analyses of the α-subunit of H,K-ATPase and ACAP4 proteins from P_1 (plasma membrane-enriched) and P_3 (tubulovesicle-enriched) fractions from resting and secreting rabbit gastric gland preparations and expressed the value as P_1/P_3 ratio. Densitometric quantitation of the α-subunit of H,K-ATPase exhibits a characteristic translocation typically seen in histamine-stimulated secreting parietal cells (11, 14, 18). Statistical analyses from four different preparations demonstrate that ACAP4 significantly translocates from cytoplasm to apical plasma membrane fraction in a pattern similar to that of H,K-ATPase (Fig. 2*E*; $p < 0.01$). We reason that ACAP4 becomes associated with the ezrin at the apical plasma membrane of secreting parietal cells.

ACAP4 Is Essential for Parietal Cell Acid Secretion—Several earlier studies established the importance of the actin-based cytoskeleton (*e.g.* see Ref. 26) and the integrity of ezrin (10) in parietal cell activation. The function of ezrin in parietal cell activation has been directly demonstrated in our recent studies (7). Given the observed interaction between ACAP4 and ezrin *in vitro* and their co-distribution *in vivo*, it was of great interest to investigate the possible influence of ACAP4 on parietal cell activation. To this end, we introduced an RNA interference oligonucleotide (siRNA 1) of ACAP4 by transfection into parietal cells. To eliminate any off target effect, we also generated an siRNA oligonucleotide targeted to a different region of ACAP4 mRNA (siRNA 2).

To determine the efficient timing for knocking down ACAP4 protein levels suppressed by the RNA interference, we transfected parietal cells with 100 nM siRNA and collected cells at different intervals of post-transfection. As shown in Fig. 3*A*, Western blot with an anti-ACAP4 antibody revealed that the siRNA 1 caused remarkable suppression of ACAP4 protein level at 48 h, whereas control cells treated with an irrelevant oligonucleotides (*e.g.* cyclophilin) express normal ACAP4 levels. Quantitative analysis revealed that the siRNA 1 treatment caused a 57.3 ± 3.1% suppression of ACAP4 protein without altering the levels of other proteins, such as ezrin. Further extension of the siRNA 1 treatment interval to 72 h did not significantly improve the efficiency of ACAP4 protein suppression. Because ACAP4 synthesis in the ~40% of untransfected cells with little or no oligonucleotide was unlikely to be markedly diminished, the observed 57% inhibition at 100 nM must represent almost complete inhibition of ACAP4 in 61 ± 3% of successfully transfected cells. Similar efficiency in ACAP4 protein suppression and specificity of the siRNA were seen in siRNA 2 (Fig. 3*B*).

TABLE 1

Vacuolar measurements in oligonucleotide-treated parietal cells

Diameters of apical vacuoles were measured as an index for apical membrane extension associated with acid secretion. Data were obtained from resting and stimulated parietal cells in which apical vacuoles were in the same focal plane. These measurements were made from three different preparations in which more than 100 cells from each category were examined. In resting cells, measurements were carried out on 3–5 vacuoles/cell of the same focal plane, whereas 1–3 vacuoles/cell were scaled in stimulated preparation. Data are expressed as mean ± S.E.

Treatment	Vacuole diameter
	μm
Resting (cimetidine)	
Scrambled siRNA 1	35 ± 0.3
Scrambled siRNA 2	3.5 ± 0.4
Ezrin siRNA 1	3.4 ± 0.5
Ezrin siRNA 2	3.5 ± 0.6
ACAP4 siRNA 1	3.6 ± 0.5
ACAP4 siRNA 2	3.6 ± 0.7
Stimulated (histamine + IBMX)	
Scrambled siRNA 1	15.9 ± 0.9
Scrambled siRNA 2	16.1 ± 1.0
Ezrin siRNA 1	5.6 ± 1.2[a]
Ezrin siRNA 2	5.3 ± 1.5[a]
ACAP4 siRNA 1	5.9 ± 1.6[b]
ACAP4 siRNA 2	6.1 ± 1.5[b]

[a] $p < 0.05$; the diameter of ezrin-suppressed histamine-treated cells was compared with that of scramble-transfected histamine-stimulated cells.

[b] $p < 0.01$ ($n = 100$ cells); the diameter of ACAP4-suppressed histamine-treated cells was significantly smaller than that of scramble-transfected histamine-stimulated cells.

Accordingly, we examined the distribution of ezrin in cultured parietal cells treated with ACAP4 siRNA oligonucleotide. Fig. 3*C* (*a′*,*b′*, and *d′*) shows optical sections taken from secreting parietal cells treated with control siRNA simultaneously probed with fluorescein-coupled ezrin antibody (*4A5*; *a*), rhodamine-conjugated anti-H,K-ATPase antibody (*b*), and Alexa Fluor 350-marked ACAP4 antibody (*ACAP4*; *c*). As seen in the control secreting parietal cells without siRNA treatment (Fig. 2*D*), the majority of ACAP4 is concentrated and co-localized with ezrin and H,K-ATPase at the apical membrane of secreting cells (Fig. 2*D*, *g* and *merge*). The ezrin distribution of ACAP4 siRNA-treated cells (Fig. 3*C*, *e*) is similar to that shown in control oligonucleotide-treated cells (Fig. 3*C*, *a*), outlining the apical membrane vacuoles with a light deposition on the basolateral membrane surface, as noted in untransfected cells (Fig. 2*D*). Although the ACAP4-containing cells produce a characteristic vacuolar swelling in response to histamine stimulation (Fig. 3*C*, *e* and *g*), suppression of ACAP4 prevents vacuolar dilation (Fig. 3*C*, *e* and *g*, *circled*). An identical phenotype was seen in parietal cells transfected with siRNA 2 (Fig. 3*D*), suggesting the potential role of ACAP4 in recruiting H,K-ATPase-containing vesicles to the apical membrane because H,K-ATPase failed to concentrate at the apical vacuoles in the ACAP4-suppressed parietal cells. Previous studies revealed that vacuole diameter can be used as a reporter for parietal cell secretory activity (7, 16). Thus, we surveyed 100 cells from resting and stimulated populations transfected with either control or ACAP4 siRNA (siRNA 1 and siRNA 2) oligonucleotides. The vacuolar measurements summarized in Table 1 show that stimulation dramatically extended vacuole diameter to 15.9 ± 0.9 μm in control oligonucleotide-treated parietal cells. However, the average vacuole diameter of ACAP4-suppressed stimulated cells was only 5.9 ± 1.6 μm (siRNA 1) and 6.1 ± 1.5 μm (siRNA 2), respectively. We therefore conclude that ACAP4 is essential for the dynamic remodeling of the apical cytoskeleton of parietal cells associated with stimulation.

To probe for the requirement of ACAP4 in parietal cell acid secretion in response to histamine stimulation, we carried out an AP uptake assay in ACAP siRNA-treated and scrambled transfected parietal cells, as described previously (16). As shown in Fig. 3*E* (*blue bars*), suppression of ACAP4 by siRNA treatment resulted in an inhibition of 89.3 ± 5.1% of acid secretion judged by the AP update ($p < 0.01$), suggesting that ACAP4 is essential for parietal cell acid secretion.

To confirm the requirement of ACAP4 for parietal cell acid secretion, we assessed the effects of overexpressing wild type ACAP4 and its GAP-deficient mutants on parietal cell acid secretion using an AP uptake assay. Typically, we achieved a 5-fold expression of exogenous proteins in positively transfected cells (10). As shown in Fig. 3*E*, overexpression of GAP-deficient ACAP4 (R469G) resulted in an inhibition of 80.5 ± 7.1% of acid secretion, judged by the AP update ($p < 0.01$). If ezrin-ACAP4 interaction is important for parietal cell activation, perturbation of such association would inhibit parietal cell secretion. Indeed, overexpression of the ezrin-binding domain of ACAP4(1–400) resulted in a 6.5-fold reduction of acid secretion. As a control, non-phosphorylatable ezrin induced a 6.8-fold reduction (~83.8 ± 7.3% inhibition) of acid secretion. In contrast, expression of wild type ACAP4 exhibited no inhibition on acid secretion, suggesting that ezrin-ACAP4 interaction is essential for parietal cell secretion.

The functional importance of ACAP4 in parietal cell secretion prompted us to examine the precise function of ezrin-ACAP4 interaction in parietal cell activation. To directly probe for the function of ezrin-ACAP4 interaction, we sought to introduce ACAP4 fragment ACAP4(1–400) into SLO-permeabilized parietal cells to disrupt endogenous ezrin-ACAP4 interaction *in vivo* using a protocol reported previously (14, 18, 20). As predicted, incubation of recombinant MBP-ACAP4(1–400) protein (5 μM) with GFP-ACAP4-bound GST-ezrin^{S66D} affinity matrix disrupts the ezrin-ACAP4 association *in vitro* (Fig. 3*F*, *lane 2*). MBP tag protein does not interfere with ezrin-ACAP4 interaction (Fig. 3*F*, *lane 1*), demonstrating the effect of ACAP4(1–400) in competing full-length ACAP4 for ezrin^{S66D} association.

If recombinant MBP-ACAP4(1–400) fusion protein disrupts endogenous ezrin-ACAP4 interaction, the addition of MBP-ACAP4(1–400) recombinant protein into SLO-permeabilized cultured parietal cells would compete for endogenous ACAP4 and retain H,K-ATPase in the cytoplasm despite the cAMP-mediated stimulation. As predicted, the majority of ACAP4 is concentrated and co-localized with ezrin and H,K-ATPase at the apical membrane of cAMP-stimulated SLO-permeabilized parietal cells in the presence of MBP protein (Fig. 3*G*, *a–c* and *merge*). Although the ezrin distribution remains associated with the apical vacuoles in ACAP4(1–400)-added cells (Fig. 3*G*, *e*), the addition of ACAP4(1–400) recombinant protein perturbs endogenous ezrin-ACAP4 interaction and prevents vacuolar dilation in response to cAMP stimulation (Fig. 3*C*, *e* and *g*, *circled*). Importantly, the cAMP-elicited H,K-ATPase translocation was also suppressed, suggesting that ACAP4 might func-

TABLE 2

Vacuolar measurements in MBP-added parietal cells

Diameters of apical vacuoles were measured as an index for apical membrane extension associated with acid secretion as described in Table 1. Data were obtained from 90 resting and stimulated parietal cells per category of three preparations in which apical vacuoles were in the same focal plane. Data are expressed as mean ± S.E.

Treatment	Vacuole diameter
	μm
Resting (cimetidine)	
MBP	37 ± 0.5
MBP-ACAP4(1–400)	3.6 ± 0.5
Stimulated (cAMP + ATP)	
MBP	15.2 ± 1.1
MBP-ACAP4(1–400)	5.3 ± 1.7[a]

[a] $p < 0.01$; the diameter of MBP ACAP4(1–400)-added cAMP-treated cells was compared with that of MBP-added cAMP-stimulated cells.

tion as a link between histamine stimulation and H,K-ATPase translocation during parietal cell activation.

To obtain quantitative analyses, we surveyed 100 cells from SLO-permeabilized parietal cells, resting and cAMP-stimulated populations, treated with MBP and MBP-ACAP4(1–400). The vacuolar measurements summarized in Table 2 show that stimulation dramatically extended vacuole diameter to 15.2 ± 1.1 μm in control MBP-added SLO-permeabilized parietal cells. However, the average vacuole diameter of MBP-ACAP4(1–400)-added cAMP-stimulated cells was only 5.3 ± 1.7 μm. We therefore conclude that ezrin-ACAP4 interaction is essential for the dynamic remodeling of the apical cytoskeleton of parietal cells in response to the cAMP stimulation.

Ezrin Specifies the Apical Localization of ACAP4—Given the observed interaction between ACAP4 and ezrin *in vitro* and their co-distribution in secreting parietal cells, it was of great interest to investigate the possible influence of ezrin on the localization of ACAP4 to the apical membrane. To this end, we introduced siRNA oligonucleotides of ezrin by transfection into parietal cells. As shown in Fig. 4, *A* and *B*, Western blotting with an anti-ezrin antibody, 4A5, revealed that 100 nM siRNA oligonucleotide (both siRNA 1 and siRNA 2) caused remarkable suppression of ezrin protein levels at 36 h. This suppression was relatively specific because it did not alter the levels of other proteins, such as ACAP4.

Accordingly, we examined the distribution of ACAP4 and H,K-ATPase in cultured parietal cells treated with ezrin siRNA. Fig. 4*C* shows optical sections taken from resting parietal cells simultaneously probed with fluorescein-conjugated anti-ezrin antibody 4A5 (*a′*), rhodamine-conjugated anti-H,K-ATPase antibody (*b′*), and Alexa Fluor 350-labeled anti-ACAP4 antibody (*d′*). The H,K-ATPase distribution of secreting parietal cells in scrambled oligonucleotide-transfected (*Control siRNA*) cells appeared identical to that of ezrin and ACAP4 staining, outlining the apical canalicular vacuole membrane (Fig. 2*D*). However, both ACAP4 and H,K-ATPase failed to concentrate at the apical vacuoles and instead exhibited a diffused distribution throughout the cytoplasm in histamine-stimulated parietal cells depleted of ezrin via transfection of siRNA 1 (Fig. 4*C*, *a′*–*c′*). An identical phenotype was seen in a different parietal cell population treated with another siRNA oligonucleotide targeted to a different region of ezrin mRNA (Fig. 4*D*), indicating that ezrin is essential for localization of ACAP4 to the apical

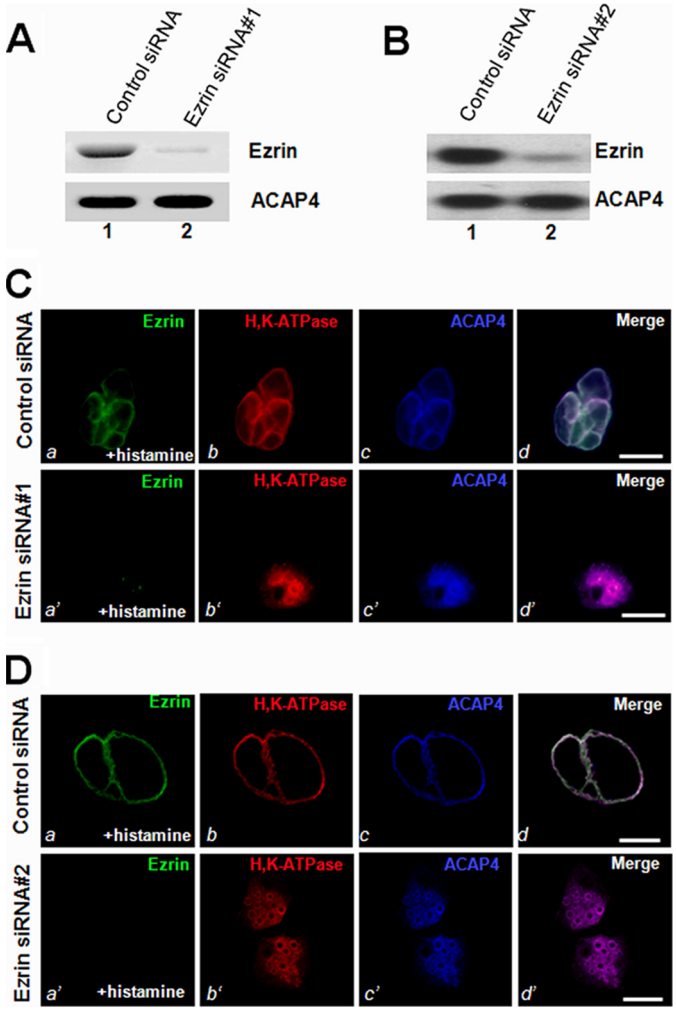

FIGURE 4. **Ezrin is essential for the apical localization of ACAP4 during parietal cell activation.** *A* and *B*, RNA interference of ezrin. Cultured parietal cells were transfected with the ezrin siRNA oligonucleotides (siRNA 1 and 2) for 36 h and subjected to SDS-PAGE and immunoblotting. *Top*, immunoblot of ezrin; *bottom*, immunoblot for ACAP4. *C* and *D*, this set of optical images was collected from gastric parietal cells treated with ezrin RNA interference oligonucleotide (siRNA 1 and 2) and triply stained for ezrin (*green*), H,K-ATPase (*red*), and ACAP4 (*blue*). In ezrin siRNA-treated secreting cells, ACAP4 staining was diffused throughout the cytoplasm. The suppression of ezrin by siRNA abolishes the apical concentration of H,K-ATPase and subsequent failure of apical membrane vacuole dilation (*b′*; *red*). However, stimulation of control siRNA-treated parietal induces a dilation of apical vacuole membrane (*a*; *green*) and concentration of H,K-ATPase to the dilated apical vacuoles. *Bar*, 15 μm.

canalicular membrane during parietal cell activation. We surveyed 100 cells from resting and stimulated populations transfected with either control or ezrin siRNA (siRNA 1 and siRNA 2) oligonucleotides. The vacuolar measurements summarized in Table 1 show that stimulation dramatically extended vacuole diameter to 15.9 ± 0.9 μm in control oligonucleotide-treated parietal cells. However, the average vacuole diameter of ezrin-suppressed stimulated cells was only 5.6 ± 1.2 μm (siRNA 1) and 5.3 ± 1.5 μm (siRNA 2), respectively. We therefore conclude that ezrin specifies ACAP4 localization to the apical membrane.

Phosphorylation of Ezrin at Ser^{66} Provides a Spatial Cue for ACAP4 Translocation in Secreting Cells—Because ezrin interacts with ACAP4 in a Ser^{66} phosphorylation-dependent man-

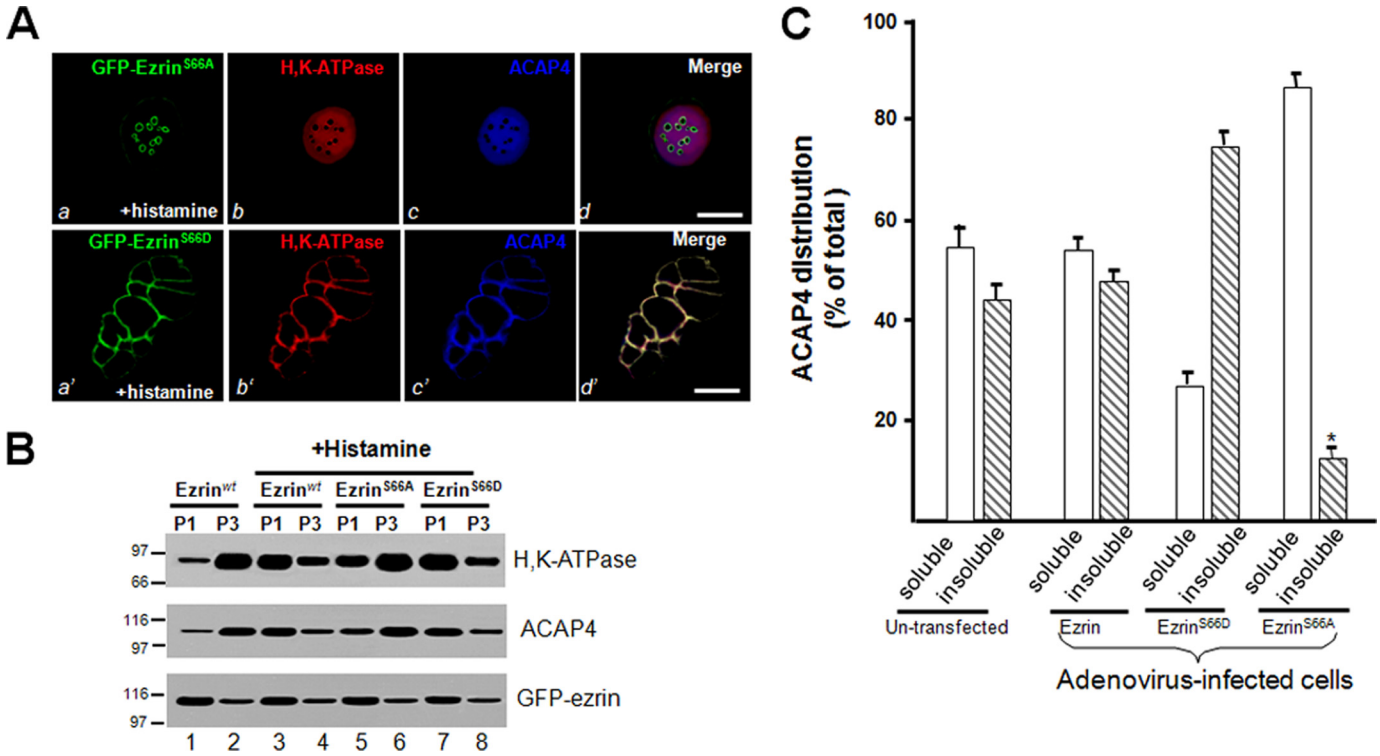

FIGURE 5. **Phosphorylation of ezrin specifies the apical localization of ACAP4.** *A*, non-phosphorylatable mutant ezrin^{S66A} blocks ACAP4 recruitment and apical membrane dilation stimulated by histamine. Expression of phospho-mimicking GFP-ezrin (*a*; *green*) outlines the dilated apical membrane in which both H,K-ATPase (*red*) and ACAP4 (*blue*) are concentrated, similar to that of endogenous ezrin (*e.g.* Fig. 3*C*, *a'–c'*). However, mutant S66A ezrin overexpression attenuates the dilation of apical vacuoles and minimizes the concentration of both H,K-ATPase (*red*) and ACAP4 (*blue*) to the apical vacuoles, demonstrating that phosphorylation of Ser^{66} is required for localization of ACAP4 to the apical membrane and apical membrane dilation. *Bar*, 15 μm. *B*, non-phosphorylatable mutant ezrin^{S66A} blocks ACAP4 recruitment from the cytoplasmic fraction to the apical membrane fraction. Aliquots of gastric glands were infected by wild type and mutant ezrin adenovirus for 12 h, followed by treatment with cimetidine or histamine plus IBMX (+*Histamine*) for 20 min at 37 °C. Treated glands were then fractionated as illustrated in Fig. 2*A*. The fractions of P_1 and P_3 were separated by SDS-PAGE, followed by Western blotting of H,K-ATPase, ACAP4, and ezrin. Note that the histamine stimulation induced a concomitant translocation of H,K-ATPase and ACAP4 from P_3 to P_1 fraction on wild type (*lanes 3* and *4*) or phospho-mimicking ezrin-infected preparations (*lanes 7* and *8*) but not non-phosphorylatable ezrin-expressing preparation (*lanes 5* and *6*), as compared with that of non-stimulated preparation (*lanes 1* and *2*). *C*, cultures of parietal cells were infected with wild type and mutant ezrin adenovirus for 12 h. Aliquots of cells were extracted with 0.1% Triton X-100 solution and separated into soluble (*s*) and insoluble (*i*) fractions. Equivalent amounts of proteins from the soluble and insoluble fractions were applied to SDS-PAGE. Following separation on 6–16% gradients, SDS-PAGE, and transblotting onto nitrocellulose membrane, the blots were probed with an anti-ACAP4 antibody and an anti-ezrin antibody 4A5 and developed with an ECL kit (Pierce). The signals were quantified using a PhosphorImager with values expressed as a percentage of the total (soluble + insoluble) and normalized to the ezrin contents. The *error bars* represent S.E.; n = 3 preparations.

ner and ACAP4 co-distributes with ezrin only in secreting cells, we reason that Ser^{66} phosphorylation may provide a spatial cue for ACAP4 translocation. To test this hypothesis, we transiently transfected cultured parietal cells to express GFP-ezrin^{S66A} and GFP-ezrin^{S66D} and assessed the distribution of ACAP4 in resting and secreting cells. As shown in Fig. 5*A*, whereas stimulation of parietal cells expressing S66D mutant ezrin produced a characteristic vacuolar swelling in response to stimulation (*a'*), cells expressing S66A ezrin displayed a morphology in which dilation of apical vacuoles is less apparent (*a*), which is consistent with previous studies (*e.g.* see Ref. 7). Similar to what was reported before, for cells expressing S66A mutant ezrin, stimulation failed to mobilize H,K-ATPase to the apical membrane because the staining remained in the cytoplasm (*b*). Examination of ACAP4 staining reveals that the majority of ACAP4 remains cytoplasmic. In contrast, expression of S66D ezrin mutant facilitates the stimulation-induced translocation of H,K-ATPase and recruitment of ACAP4 to the apical membrane (Fig. 5*D*, *b'* and *c'*).

To validate that phosphorylation of ezrin at Ser^{66} is essential for relocation of ACAP4 in secreting parietal cells, we carried out membrane fractionation experiments on glands maintained in the resting state with cimetidine and glands that were infected with GFP-ezrin adenovirus for 4 h prior to histamine stimulation. Homogenates of the variously treated gland preparations were separated by differential centrifugation, and cell fractions were assayed for H,K-ATPase content for validating the stimulation of acid secretion. As shown in Fig. 5*B*, ACAP4 and H,K-ATPase reside in microsomal fraction P_3 of resting cells (*lane 3*) and relocated to the apical membrane fraction of secreting cells (*lane 4*), whereas the GFP-ezrin level remained unchanged in P_1 and P_3 in response to histamine stimulation (*bottom*, *lanes 2* and *4*). However, overexpression of non-phosphorylatable ezrin^{S66A} prevents translocation of H,K-ATPase, consistent with our previous observation (7). As predicted, ACAP4 translocation is also arrested in parietal cells overexpressing non-phosphorylatable ezrin^{S66A}, demonstrating the importance of phosphorylation of ezrin at Ser^{66} for ACAP4 targeting. In supporting this notion, overexpression of phospho-mimicking ezrin^{S66D} facilitates the translocation of ACAP4 and H,K-ATPase. Quantitative Western blotting analyses confirmed that phosphorylation of Ser^{66} is essential for retaining

ACAP4 in the Triton X-100-insoluble "cytoskeletal" fraction (Fig. 5*C*), suggesting that ACAP4 binds tightly to ezrin^{S66D}. We therefore conclude that PKA-mediated phosphorylation of ezrin at Ser^{66} provides a spatial cue essential for ACAP4 docking to the apical canalicular membrane and subsequent proton pump translocation to the apical membrane.

DISCUSSION

Ezrin, a founding member of the membrane-cytoskeleton linker of the ezrin/radixin/moesin protein family, has been implicated in a variety of volatile membrane-cytoskeletal dynamics, including cell migration, immunological synapse formation, and regulated exocytosis (*e.g.* see Ref. 2). Here we provide the first evidence that ezrin interacts with ACAP4, an ARF6 GTPase-activating protein containing a pleckstrin homology domain and ankyrin repeats (10). Although our early study revealed that ezrin-ACAP4 form a volatile membrane regulatory complex, their physical interaction was never demonstrated. ACAP4 binds to ezrin via its N-terminal 400 amino acids and is co-localized with ezrin to the apical membrane of secreting parietal cells. Furthermore, our studies show that Ser^{66}-phosphorylated ezrin is essential for the apical localization of ACAP4 because either suppression of ezrin phosphorylation or deletion of the ezrin eliminates the apical targeting of ACAP4. Finally, our studies demonstrate the essential role of ezrin-ACAP4 interaction in the apical membrane remodeling associated with parietal cell secretion.

An essential role for the actin cytoskeleton in the secretory processes of parietal cells has been inferred from studies using actin disruptors that disorganize actin filaments and act to inhibit acid secretion (22). Highly organized microfilaments are typical features of microvilli at the apical membrane within the parietal cell canaliculus. In going from the resting to the secreting state, there are major changes at the apical canalicular surface, including elongation of microvilli. Interestingly, as the parietal cell returns to the resting state after withdrawal of stimulants, microfilament ultrastructural changes become apparent as a disorganization of actin filaments along with collapse of the apical canalicular surface (25, 27). These morphological studies indicate that reversible actin-based cytoskeletal dynamics are tightly linked to the secretory cycle in parietal cells. Gastric ezrin was initially identified as a PKA substrate associated with parietal cell acid secretion (28). Both cellular and animal experiments demonstrated the essential role of ezrin in gastric acid secretion (7, 8). Our recent studies demonstrate that ezrin couples PKA-mediated phosphorylation to the remodeling of the apical membrane cytoskeleton associated with acid secretion in parietal cells (7). However, knowledge of how ezrin operates H,K-ATPase trafficking upon the parietal cell activation by histamine stimulation has remained elusive.

ARF6 GTPase is a conserved regulator of membrane trafficking and actin-based cytoskeleton dynamics at the leading edge of migrating cells. A key determinant of ARF6 function is the lifetime of the GTP-bound active state, which is orchestrated by GAP and GTP-GDP exchanging factor. To systematically analyze proteins that regulate ARF6 activity during volatile membrane dynamics, we performed a proteomic analysis of proteins selectively bound to active ARF6 using mass spectrometry and identified a novel ARF6 complex containing PALS1, calpain, ezrin, and ACAP4. ACAP4 encodes 903 amino acids and contains two coiled coils, one pleckstrin homology domain, one GAP motif, and two ankyrin repeats. Our biochemical characterization demonstrated that ACAP4 has a phosphatidylinositol 4,5-bisphosphate-dependent GAP activity specific for ARF6. The co-localization of ACAP4 with ARF6 occurred in ruffling membranes formed upon epidermal growth factor stimulation. Significantly, the depletion of ACAP4 by small interfering RNA or inhibition of ARF6 GTP hydrolysis by overexpressing GAP-deficient ACAP4 suppressed cell migration in wound healing, demonstrating the importance of ACAP4 in volatile membrane-cytoskeleton remodeling.

Our present study shows that phospho-Ser^{66} provides a spatiotemporal cue for tubulovesicle membrane trafficking to the apical membrane via a site-specific phosphorylation-dependent ezrin-ACAP4 interaction. It is worth noting that ezrin is an interacting protein of the regulatory subunit of PKA that is implicated in the apical localization of PKA (29). Thus, the interaction between phosphoezrin and ACAP4 established here may organize an apical signaling complex that orchestrates membrane recruitment and membrane cytoskeletal reorganization. Precise mapping of respective binding interfaces between these three proteins will aid in delineating the molecular mechanisms underlying polarity establishment and/or maintenance in gastric parietal cells. In addition, it would be of great interest to visualize the PKA spatiotemporal dynamics of parietal cells in response to histamine stimulation.

Our early study showed that WWOX interacts with ezrin via the polyproline region located at the C terminus of ezrin and is required for gastric parietal cell secretion (12). Although both WWOX and ACAP4 interact with ezrin in a phosphorylation-dependent manner and are required for parietal cell activation, they interact with ezrin via different regions and function at different steps of parietal cell activation. In addition, those two proteins interact with different structures of ezrin. Our preliminary studies suggest that ACAP4-ezrin interaction is essential for tubulovesicle docking to the apical membrane, whereas WWOX functions as a priming step for fusion of the tubulovesicle membrane with the apical plasma membrane.[4] It would be of great interest to apply supraresolution microscopy, such as photoactivated localization microscopy, to visualize how WWOX and ACAP4 molecules facilitate the apical membrane remodeling underlying parietal cell activation.

Parietal cell activation involves translocation of H,K-ATPase from the cytoplasm to the apical plasma membrane via multiple steps, including the possible trafficking over actin filaments, docking to secretory sites, insertion of the pump into the apical membrane, and perhaps maintenance of the pump in the apical membrane during active secretion. Recent studies show that ARF6 regulates gastric acid secretion in parietal cells and that the GTP hydrolysis cycle of ARF6 is essential for the activation pathway (9). However, it was unclear at that time how ARF6 translocates to the apical secretory membrane upon stimulation. Our studies suggest that ARF6-ACAP4-ezrin may

[4] X. Ding and X. Yao, unpublished observation.

constitute an apical signaling complex that coordinates the respective roles of actin-based cytoskeleton and membrane fusion machinery in mediating H,K-ATPase translocation to the apical membrane, it remains to be established how ARF6-ACAP4-ezrin interaction operates the apical membrane cytoskeletal dynamics to facilitate the docking and insertion of H,K-ATPase to the apical membrane of parietal cells for proton pumping. In this regard, molecular illustration of PKA kinase gradient and ARF6 activation dynamics during parietal cell activation will facilitate a better understanding of gastric parietal cell physiology.

Phosphorylation of ezrin has been functionally linked to membrane dynamics and plasticity. Our previous study demonstrated that phosphorylation of the conserved Thr^{567} residue of ezrin alters the physiology of gastric parietal cells (30). We have recently established a protocol in which phosphorylation-mediated protein conformational change can be studied at the single molecule level (31). Using this protocol, we have correlated phosphorylation-induced conformational change of ezrin-Thr^{567} with its functional activity in cellular localization. Using the same protocol, our preliminary study shows that phosphorylation of ezrin at Ser^{66} also unfolds ezrin intramolecular association. Although Thr^{567} phosphorylation retains the N-terminal globular domain of ezrin half-folded (31), Ser^{66} phosphorylation fully extends the ezrin molecule. Precise comparative analyses are under way to provide a molecular illustration of phosphorylation-elicited functional activation of ezrin and delineate how stimulus-induced protein conformational change is used as a signaling mechanism orchestrating cellular dynamics.

Taken together, the present work reveals that phosphoezrin interacts with an ARF6 GTPase-activating protein, ACAP4, and that this interaction specifies the apical localization of ACAP4. Finally, we show that disruption of ezrin-ACAP4 interaction blocks the remodeling of the apical membrane cytoskeleton associated with the translocation and insertion of H,K-ATPase to the apical membrane. We propose that ACAP4-ezrin interaction links proton pump H,K-ATPase trafficking to apical membrane- cytoskeletal remodeling required for polarized secretion in gastric parietal cells.

Acknowledgments—We thank members of our groups for insightful discussion during the course of this study and Professor John Forte for artwork.

REFERENCES

1. Yeaman, C., Grindstaff, K. K., Hansen, M. D., and Nelson, W. J. (1999) *Curr. Biol.* **9,** R515–R517
2. Bretscher, A., Edwards, K., and Fehon, R. G. (2002) *Nat. Rev. Mol. Cell Biol.* **3,** 586–599
3. Urushidani, T., Hanzel, D. K., and Forte, J. G. (1989) *Am. J. Physiol.* **256,** G1070–G1081
4. Yao, X., and Forte, J. G. (2003) *Annu. Rev. Physiol.* **65,** 103–131
5. Yao, X., Chaponnier, C., Gabbiani, G., and Forte, J. G. (1995) *Mol. Biol. Cell* **6,** 541–557
6. Yao, X., Cheng, L., and Forte, J. G. (1996) *J. Biol. Chem.* **271,** 7224–7229
7. Zhou, R., Cao, X., Watson, C., Miao, Y., Guo, Z., Forte, J. G., and Yao, X. (2003) *J. Biol. Chem.* **278,** 35651–35659
8. Tamura, A., Kikuchi, S., Hata, M., Katsuno, T., Matsui, T., Hayashi, H., Suzuki, Y., Noda, T., Tsukita, S., and Tsukita, S. (2005) *J. Cell Biol.* **169,** 21–28
9. Matsukawa, J., Nakayama, K., Nagao, T., Ichijo H., and Urushidani, T. (2003) *J. Biol. Chem.* **278,** 36470–36475
10. Fang, Z., Miao, Y., Ding, X., Deng, H., Liu, S., Wang, F., Zhou, R., Watson, C., Fu, C., Hu, Q., Lillard, J. W., Jr., Powell, M., Chen, Y., Forte, J. G., and Yao, X. (2006) *Mol. Cell Proteomics* **5,** 1437–1449
11. Hanzel, D. K., Urushidani, T., Usinger, W. R., Smolka, A., and Forte, J. G. (1989) *Am. J. Physiol.* **256,** G1082–G1089
12. Jin, C., Ge, L., Ding, X., Chen, Y., Zhu, H., Ward, T., Wu, F., Cao, X., Wang, Q., and Yao, X. (2006) *Biochem. Biophys. Res. Commun.* **341,** 784–791
13. Yao, X., Thibodeau, A., and Forte, J. G. (1993) *Am. J. Physiol.* **265,** C36–C46
14. Ammar, D. A., Zhou, R., Forte, J. G., and Yao, X. (2002) *Am. J. Physiol. Gastrointest. Liver Physiol.* **282,** G23–G33
15. Bradford, M. M. (1976) *Anal. Biochem.* **72,** 248–254
16. Cao, X., Ding, X., Guo, Z., Zhou, R., Wang, F., Long, F., Wu, F., Bi, F., Wang, Q., Fan, D., Forte, J. G., Teng, M., and Yao, X. (2005) *J. Biol. Chem.* **280,** 13584–13592
17. Yao, X., Karam, S. M., Ramilo, M., Rong, Q., Thibodeau, A., and Forte, J. G. (1996) *Am. J. Physiol.* **271,** C61–C73
18. Ding, X., Wu, F., Guo, Z., and Yao, X. (2008) *Methods Mol. Biol.* **440,** 217–226
19. Urushidani, T., and Forte, J. G. (1987) *Am. J. Physiol.* **252,** G458–G465
20. Goldenring, J. R., Soroka, C. J., Shen, K. R., Tang, L. H., Rodriguez, W., Vaughan, H. D., Stoch, S. A., and Modlin, I. M. (1994) *Am. J. Physiol.* **267,** G187–94
21. Lou, Y., Yao, J., Zereshki, A., Dou, Z., Ahmed, K., Wang, H., Hu, J., Wang, Y., and Yao, X. (2004) *J. Biol. Chem.* **279,** 20049–20057
22. Berryman, M., Franck, Z., and Bretscher, A. (1993) *J. Cell Sci.* **105,** 1025–1043
23. Zhu, L., Hatakeyama, J., Zhang, B., Makdisi, J., Ender, C., and Forte, J. G. (2009) *Am. J. Physiol. Gastrointest. Liver Physiol.* **296,** G185–G195
24. Wang, F., Xia, P., Wu, F., Wang, D., Wang, W., Ward, T., Liu, Y., Aikhionbare, F., Guo, Z., Powell, M., Liu, B., Bi, F., Shaw, A., Zhu, Z., Elmoselhi, A., Fan, D., Cover, T. L., Ding, X., and Yao, X. (2008) *J. Biol. Chem.* **283,** 26714–26725
25. Forte, T. M., Machen, T. E., and Forte, J. G. (1977) *Gastroenterology* **73,** 941–955
26. Zhou, R., Zhu, L., Kodani, A., Hauser, P., Yao, X., and Forte, J. G. (2005) *J. Cell Sci.* **118,** 4381–4391
27. Black, J. A., Forte, T. M., and Forte, J. G. (1982) *Gastroenterology* **83,** 595–604
28. Forte, J. G., and Yao, X. (1996) *Trends Cell Biol.* **6,** 45–48
29. Urushidani, T., Hanzel, D. K., and Forte, J. G. (1987) *Biochim. Biophys. Acta* **930,** 209–219
30. Dransfield, D. T., Bradford, A. J., Smith, J., Martin, M., Roy, C., Mangeat, P. H., and Goldenring, J. R. (1997) *EMBO J.* **16,** 35–43
31. Liu, D., Ge, L., Wang, F., Takahashi, H., Wang, D., Guo, Z., Yoshimura, S., Ward, T., Ding, X., Takeyasu, K., and Yao, X. (2007) *FEBS Lett.* **581,** 3563–3571